Modelling carbon assimilatory and recycling pathways in *Arabidopsis* seedlings

Problem presented by

Elizabeth Allen, Mark Hooks, Bangor University,
e.j.allen@bangor.ac.uk m.a.hooks@bangor.ac.uk

at the 2nd Mathematics in the Plant Sciences Study Group,
Nottingham, 5–8 January, 2009

Contributors

Martin Berglund, Chalmers, Sweden, martin.berglund@chalmers.se
Hilmar Castro, Venezuela, hcastro@usb.ve
Anna Lovrics, Nottingham, anna.lovrics@maths.nottingham.ac.uk
Tal Pearson, Nottingham, pmxtp@nottingham.ac.uk
Nikolas Popovich, Edinburgh, Nikola.Popovic@ed.ac.uk
Jamie Twycross, Nottingham, jpt@cpib.ac.uk
Maria Grazia Vigliotti, Imperial College, mgv98@doc.ic.ac.uk
Minaya Villasania, Nottingham, mdv@cs.nott.ac.uk
Jonathan Wattis, Jonathan.Wattis@nottingham.ac.uk

Report compiled by

Jonathan Wattis, Jonathan.Wattis@nottingham.ac.uk
Mark Hooks, Bangor University, m.a.hooks@bangor.ac.uk
Jamie Twycross, Nottingham, jpt@cpib.ac.uk
Anna Lovrics, Nottingham, anna.lovrics@maths.nottingham.ac.uk

July 24, 2009

Contents

1 Introduction

1.1 Motivation

Seeds become primed for the process of germination following imbibition (taking up fluid). Unless environmental factors and genetic factors impede this process at a very early stage through dormancy, germination is a nonreversible process with the ultimate goal of producing a fully photosynthetic seedling. In order to support the growth of the newly germinated seedling, a seed's lipid stores are mobilized and either converted into sugars for transport to sink tissues or respired for energy [7]. Early research on the castor bean system demonstrated the involvement of the glyoxylate cycle to take acetyl-CoA from β-oxidation and convert it into organic acids for transport to the mitochondria, the switch-house between sugar formation and respiration [1].

Work with castor bean implicated succinate as the singular step in transfer of carbon from peroxisome to mitochondria [1]. More recent work on the model plant *Arabidopsis* has confirmed that for the β-oxidation to occur, other organic acids, particularly citrate [11], and malate [12, 14], are exported from the peroxisome. These could potentially contribute to anapleurotic and gluconeogenic carbon supply. The characterization of mutants in both β-oxidation and the glyoxylate cycle has identified critical steps in fatty acid mobilization, that when disrupted, prevent fatty acid mobilization and even seedling development [12]. However, elimination of the unique enzymes of the glyoxylate cycle isocitrate lyase [4] and malate synthase [3] in *Arabidopsis* appear to affect lipid mobilization and seedling development under suboptimal growth conditions. Such results have led to the conclusion that citrate is the major organic acid transported to mitochondria [11]. There are alternative uses for both citrate and malate, the former contributes to cytosolic acetyl-CoA formation through the ATP citrate lyase [6], and the latter is partitioned between oxaloacetic acid (denoted OAA, for re-entry into the peroxisome) and entry into the citric acid cycle (also known as the tricarboxylic cycle, which we will refer by the acronym TCA).

The feeding studies conducted on *Arabidopssis* so far have used primarily labelled acetate to represent the pool of acetyl-CoA coming from β-oxidation. Through a forward genetic screen using the toxic acetate analogue monofluoroacetic acid, the transport and acetate activation steps were discovered and shown to reduce the flow of acetate into soluble carbohydrates by as much as 75% [8, 13]. Since these steps lie outside the normal pathways involved in lipid mobilization, it can be hypothesized that no effect on metabolism in seedlings would be apparent. However, elimination of the activation step resulted in faster establishing seedlings and a dramatic ($\sim$50%) decrease in primary metabolite levels, including soluble sugars, amino acids and organic acids that would come from the fatty acid derived acetyl-CoA [personal communication, Allen & Hooks]. Interestingly, it was observed that acetate levels were lower and acetyl-CoA levels were higher in the mutant (*acn1*) than in the corresponding wildtype, which was counterintuitive to the function of the missing acetyl-CoA synthetase activity. Based on these intriguing results, it would be highly beneficial to formulate mathematical models that could explain these observations and reveal subsequent points of experimentation to unravel carbon flows in establishing seedlings.

1.2 Background biology

If we track the amount of fatty acids in the seedling, we find that it takes a day or two before it is used in any appreciable quantity, then between days two to four it is used at an almost constant rate. After day four the use of fatty acids is reduced as it becomes depleted and photosynthesis starts to provide energy for the seedling. The activity of the glyoxysome cycle also takes a day or two to become fully activated; and then between days two to four it is operating at a maximal rate, and following day four its activity reduces. This behaviour is illustrated in Figure 1, which illustrates the data shown in Figure 5 of [4]. Hence from days two to four we observe the seedling is in an approximate steady-state, with constant (time-independent) fluxes through all pathways. In the analysis of the model presented later (section 3) we shall make use of steady-state assumptions to simplify the results derived.

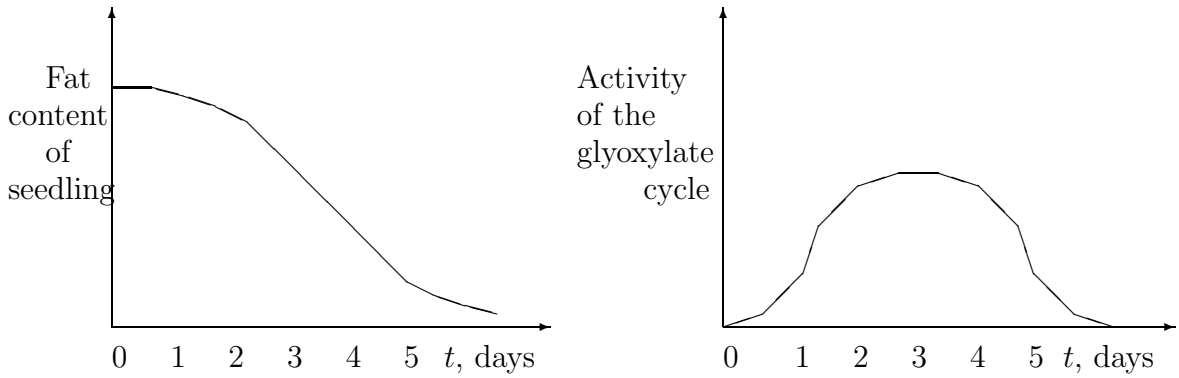

Figure 1: Illustration of the usage of fats (left) and the activity of glyoxylate cycle (right) over time. The activity of glyoxylate cycle is assumed from the activity profiles of the unique enzymes isocitrate lyase and malate synthase.

Figure 2 shows one simplification of the metabolic pathways active during the first week of a seedling's growth. This shows that following the transport of fatty acids into the glyoxysome they are systematically catabolised through the β-oxidation cycle producing acetyl-coA. We assume that this is part of the same pool of acetyl-coA in the glyoxysome as that which arrives due to acetate being transported across the membrane and then being converted into acetyl-coA. The glyoxylate cycle operates in the glyoxysome producing succinate, the gluconeogenic precursor according to classic models of glyoxylate cycle function.

In addition to the above, Figure 3 shows that acetyl-coA in the cytosol leads to biosynthesis. Furthermore, carbohydrate and the citric acid cycle (TCA) in mitochondria also lead to biosynthesis, amino acids and polyamines in the cytosol. Figure 3 shows two variants of the pathway diagram: one for wildtype *Arabidopsis* (Columbia-7) which has an enzyme which converts acetate to acetyl-CoA in the glyoxysome. The mutant *acn1* does not have this enzyme. Lack of this enzyme would permit peroxisomal thioesterase activity to become significant for hydrolysis of acetyl-CoA. Also, it is hypothesised that the wild type exhibits inhibition of biosynthetic processes and of carbohydrate catabolic pro-

cesses through catabolite repressive mechanisms as suggested by gene expression changes in the mutant (Allen & Hooks, personal communication).

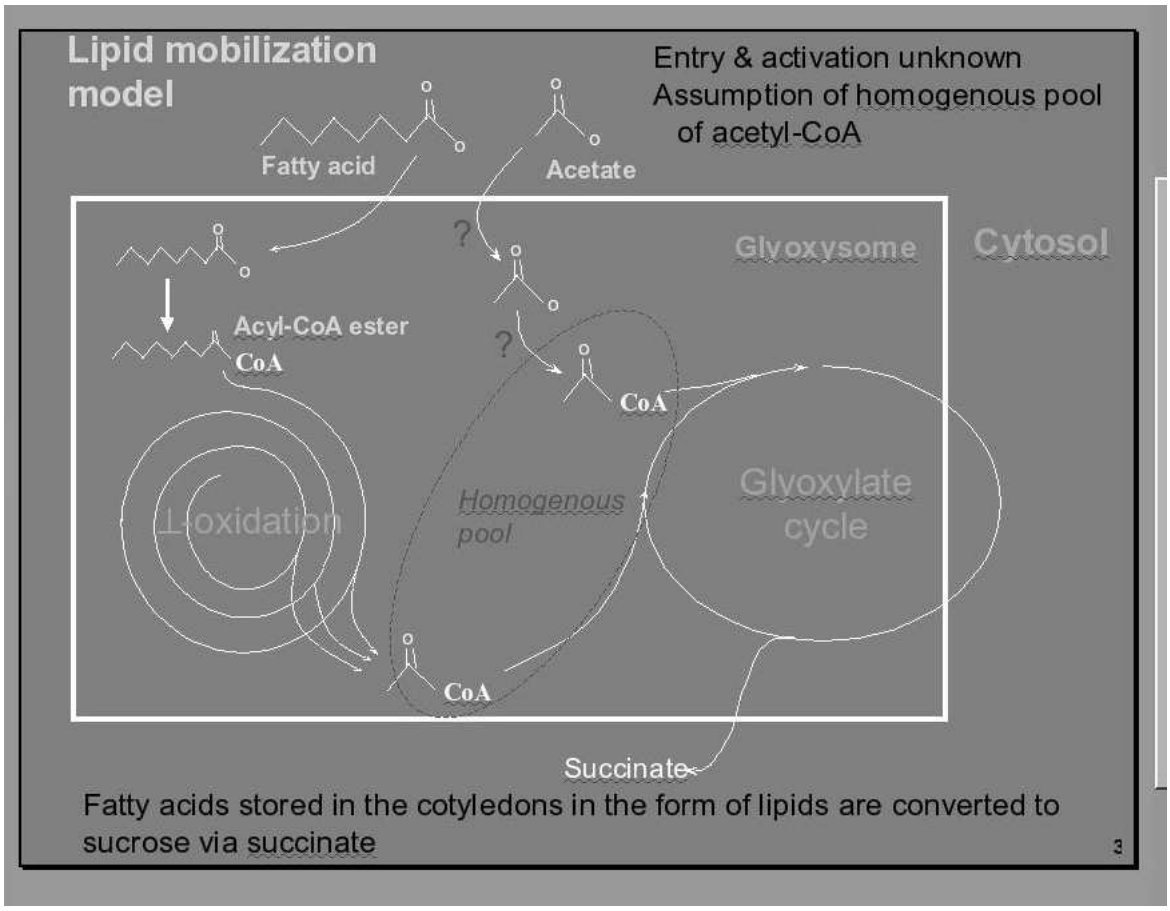

Figure 2: Illustration of the classic pathway of lipid mobilization in oilseeds showing the placement of acetate and acetyl-CoA within the scheme.

Chemical Species	Wildtype (Col-7)	*acn1-2*
Total acetate	45 ± 6	16 ± 8
Total acetyl-CoA	38 ± 35	88 ± 18

Table 1: Table of experimental data from metabolite profiles taken three days post-imbibition, showing that free acetate is higher in the wildtype and acetyl-CoA is higher in the mutant.

There follows a list of questions which we hoped would be addressable by a mathematical modelling approach:

1. Why is free acetate not accumulating within the *acn1* mutant, but acetyl-CoA does?

2. Why does the elimination of ACN1 have a large reductive effect on metabolite levels?

3. Does acetyl-CoA from free acetate mimic acetyl-CoA pools derived from fatty acid catabolism?

4. Must acetate and fatty acids share common metabolic pathways and isozymes?

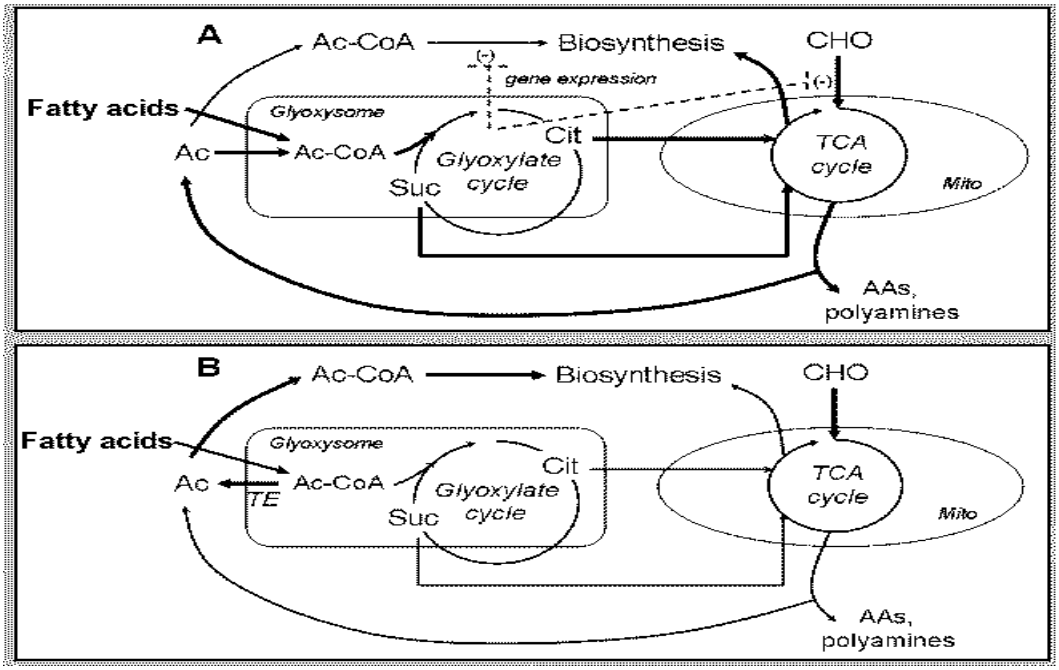

Figure 3: The two metabolic pathway diagrams for the wildtype (A) and the mutant *acn1* (B). In (A) we have the enzyme which converts acetate to acetyl-CoA in the glyoxysome, this is missing or nonfunctional in the mutant. Also absent from the mutant is potential inhibition of carbohydrate (CHO) respiration by the citric acid cycle (TCA) and entry of acetyl-CoA into the biosynthetic pathways. Net transport of acetyl-CoA out of the glyoxysome *via* acetate by TE becomes a possibility in the mutant lacking ACN1.

5. What, if any, is the contribution of acetate recycling to metabolite levels?

6. What is the contribution of cytosolic sources to free acetate and acetyl-CoA levels?

2 Model

The goal for the modelling group was to determine if mathematical models could be derived to fit the observation on differences in acetate, acetyl-CoA, and metabolite levels in the *acn1* mutant compared to the wildtype by taking into account those assumptions outlined in the Background biology above (§1.2). In Figure 4, we have combined the information of Figures 2 and 3 into one flowchart which includes all the processes active in both the wildtype and the mutant *acn1*.

We use the law of mass action to model the chemical reactions in each of the two compartments (with subscripts of g and c respectively for the glyoxysome and the cytosol). Equations for the total numbers of molecules of each species in each compartment can be written down, and are then converted to concentrations by dividing by the volume of each compartment. We divide each equation by the volume of the glyoxysome, which introduces a volume ratio $v = V_{\text{cytosol}}/V_{\text{glyoxysome}}$.

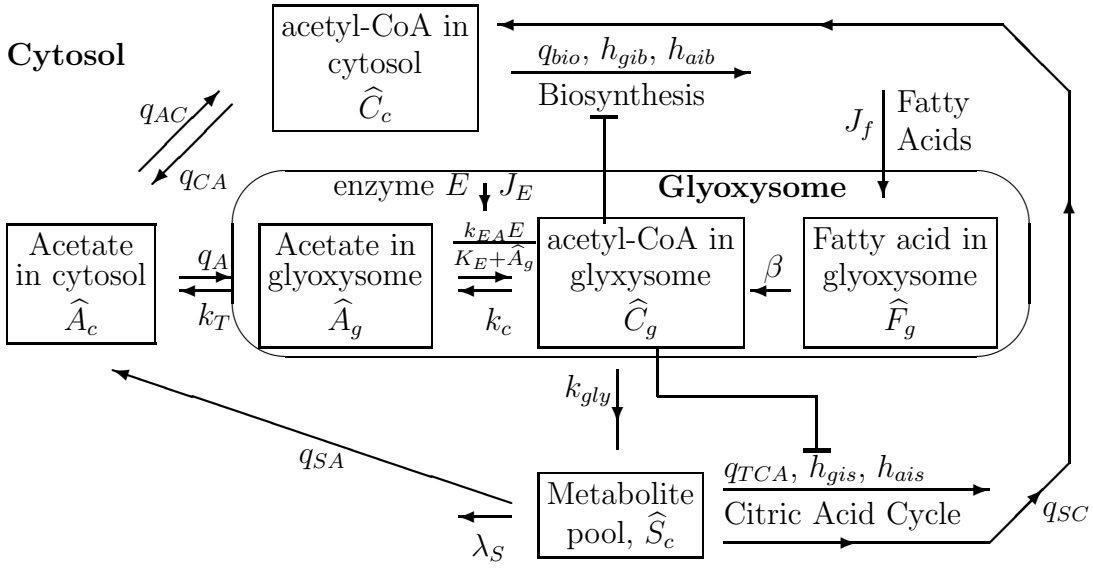

Figure 4: Illustration of pathways modelled in this report. Not all the pathways are active in both the wildtype and the mutant (*acn1*).

Using hatted variables for dimensional concentrations, we combine the transport processes between the two compartments with the reactions occurring in each compartment using ordinary differential equations, representing the model by

$$\underbrace{\frac{\mathrm{d}\widehat{F}_g}{\mathrm{d}\widehat{t}}}_{\substack{\text{rate of}\\ \text{change of}\\ \text{fatty acid}}} = \underbrace{J_f \exp(-\Gamma\widehat{t})}_{\substack{\text{transport of}\\ \text{fatty acid into}\\ \text{glyoxysome}}} - \underbrace{\beta\widehat{F}_g}_{\substack{\text{loss of fat}\\ \text{by } \beta\text{-oxidation}}}, \tag{1}$$

$$\underbrace{\frac{\mathrm{d}\widehat{A}_g}{\mathrm{d}\widehat{t}}}_{\substack{\text{rate of change}\\ \text{of acetate in}\\ \text{glyoxysome}}} = \underbrace{k_c\widehat{C}_g}_{\substack{\text{conversion}\\ \text{of coA to}\\ \text{acetate}}} - \underbrace{\frac{k_{EA}\widehat{A}_g\widehat{E}}{K_E+\widehat{A}_g}}_{\substack{\text{enzymatic}\\ \text{conversion of}\\ \text{acetate to coA}}} - \underbrace{k_T\widehat{A}_g}_{\substack{\text{TE-export}\\ \text{of acetate}\\ \text{(in mutant)}}} + \underbrace{q_A\widehat{A}_c}_{\substack{\text{transport of}\\ \text{acetate into}\\ \text{glyoxysome}}} \tag{2}$$

$$\underbrace{\frac{\mathrm{d}\widehat{C}_g}{\mathrm{d}\widehat{t}}}_{\substack{\text{rate of}\\ \text{change}\\ \text{of coA}}} = \underbrace{\beta\widehat{F}_g}_{\substack{\text{production}\\ \text{of coA via}\\ \beta\text{-oxidation}}} + \underbrace{\frac{k_{EA}\widehat{A}_g\widehat{E}}{K_E+\widehat{A}_g}}_{\substack{\text{enzymatic}\\ \text{production}\\ \text{of coA}}} - \underbrace{k_c\widehat{C}_g}_{\substack{\text{conversion}\\ \text{of coA}\\ \text{to acetate}}} - \underbrace{k_{gly}\widehat{C}_g}_{\substack{\text{coA enters}\\ \text{glyoxylate}\\ \text{cycle}}}, \tag{3}$$

$$\underbrace{\frac{\mathrm{d}\widehat{E}}{\mathrm{d}\widehat{t}}}_{\substack{\text{rate of}\\ \text{change of}\\ \text{enzyme}}} = \underbrace{J_E}_{\substack{\text{constant}\\ \text{production}\\ \text{of enzyme}}}, \tag{4}$$

in the glyoxysome, and, in the cytosol, by

$$\underbrace{v\frac{\mathrm{d}\widehat{A}_c}{\mathrm{d}\widehat{t}}}_{\substack{\text{rate of}\\ \text{change of}\\ \text{acetate}}} = \underbrace{k_T\widehat{A}_g}_{\substack{\text{TE-export}\\ \text{of acetate}\\ \text{(in mutant)}}} - \underbrace{q_A\widehat{A}_c}_{\substack{\text{loss of}\\ \text{acetate to}\\ \text{glyoxysome}}} - \underbrace{q_{AC}\widehat{A}_c}_{\substack{\text{conversion}\\ \text{of acetate}\\ \text{to coA}}} + \underbrace{q_{CA}\widehat{C}_c}_{\substack{\text{conversion}\\ \text{of coA to}\\ \text{acetate}}} + \underbrace{q_{SA}\widehat{S}_c}_{\substack{\text{recycling of}\\ \text{metabolites}\\ \text{to acetate}}}, \tag{5}$$

$$\underbrace{v\frac{\mathrm{d}\widehat{C}_c}{\mathrm{d}\widehat{t}}}_{\substack{\text{rate of}\\ \text{change}\\ \text{of coA}}} = \underbrace{q_{AC}\widehat{A}_c}_{\substack{\text{conversion}\\ \text{of acetate}\\ \text{to coA}}} - \underbrace{q_{CA}\widehat{C}_c}_{\substack{\text{conversion}\\ \text{of coA to}\\ \text{acetate}}} - \underbrace{\frac{q_{bio}\widehat{C}_c}{1+h_{gib}k_{gly}\widehat{C}_g+h_{aib}\widehat{A}_c}}_{\text{biosynthesis}} + \underbrace{q_{SC}\widehat{S}_c}_{\substack{\text{conversion of}\\ \text{metabolites}\\ \text{to coA}}}, \tag{6}$$

$$\underbrace{v\frac{\mathrm{d}\widehat{S}_c}{\mathrm{d}\widehat{t}}}_{\substack{\text{rate of}\\ \text{change of}\\ \text{metabolites}}} = \underbrace{k_{gly}\widehat{C}_g}_{\substack{\text{from}\\ \text{glyoxylate}\\ \text{cycle}}} - \underbrace{\frac{q_{TCA}}{1+h_{gis}k_{gly}\widehat{C}_g+h_{ais}\widehat{A}_c}}_{\substack{\text{production from}\\ \text{carbohydrates via}\\ \text{mitochondria}}} - \underbrace{(q_{SA}+q_{SC})\widehat{S}_c}_{\substack{\text{recycling}\\ \text{to coA \&}\\ \text{acetate}}} - \underbrace{\lambda_S\widehat{S}_c}_{\substack{\text{energy}\\ \text{usage in}\\ \text{seedling}}}. \tag{7}$$

Here, v is the nondimensional volume ratio of the cytosol to the glyoxysome (hence $v \gg 1$). This is estimated by $v = 30$, using a cell volume of 1 pl and assuming the volume of the glyoxysome is in the range 10–100 fl. The parameters are summarised in Table 2. Initially all parameters were set to unity, and then certain parameters were varied in order to fit the data qualitatively to expected behaviour. The initial conditions we use for the system (1)–(7) are

$$F_g(0) = F_0, \quad A_g(0) = 0, \quad C_g(0) = 0, \tag{8}$$

$$E(0) = 0, \quad A_c(0) = 0, \quad C_c(0) = 0, \quad S_c(0) = 0. \tag{9}$$

2.1 Nondimensionalisation of model

We nondimensionalise the variables according to

$$\widehat{t} = \frac{t}{\beta}, \qquad \widehat{F}_g = \frac{J_f F_g}{\beta}, \qquad \widehat{C}_g = \frac{J_f C_g}{k_{gly}}, \qquad \widehat{E} = \frac{J_E E}{\beta}, \qquad \widehat{A}_g = \frac{J_f q_{CA} A_g}{k_{gly} q_{AC}},$$

$$\widehat{C}_c = \frac{J_f q_{AC} q_{SA} C_c}{q_{CA} q_A (\lambda_S + q_{SA} + q_{SC})}, \quad \widehat{A}_c = \frac{J_f q_{SA} A_c}{q_A (\lambda_S + q_{SA} + q_{SC})}, \quad \widehat{S}_c = \frac{J_f S_c}{(\lambda_S + q_{SA} + q_{SC})}, \tag{10}$$

Parameter	Explanation	Value
v	Ratio of cytosol volume to glyoxysome volume	30
J_f	Amount of Fatty Acid store is depleted	1
Γ	Rate at which Fatty Acid store is depleted	300
β	Rate of β-oxidation	1
k_c	Rate of conversion of acetyl-CoA into acetate in glyoxysome	10
k_{EA}	Rate of conversion of acetate into acetyl-CoA in glyoxysome	0.01
K_E	Michaelis-menten constant	0.01
k_T	Rate of export of acetate from glyoxylate	0 or 130
q_A	Rate of transport of acetate into glyoxysome	1.5
k_{gly}	Rate of conversion of C_g to metabolites	10
J_E	Rate of enzyme production	4
q_{AC}	Rate of conversion of acetate to acetyl-CoA in cytosol	5
q_{CA}	Rate of conversion of acetyl-CoA to acetate in cytosol	0
q_{SC}	Rate of recycling of metabolites to acetyl-CoA	0
λ_S	Use of metabolites for energy	10
q_{TCA}	Rate at which metabolites enter Citric Acid cycle	1
q_{bio}	Rate at which acetyl-CoA enters biosynthesis	3
h_{gis}	Inhibitory effect of C_g on citric acid cycle	0
h_{ais}	Inhibitory effect of A_c on citric acid cycle	0
h_{gib}	Inhibitory effect of C_g on biosynthesis	0
h_{aib}	Inhibitory effect of A_c on biosynthesis	0

Table 2: Table of dimensional parameters.

then

$$\frac{\mathrm{d}F_g}{\mathrm{d}t} = \exp(-\gamma t) - F_g, \qquad \frac{\mathrm{d}E}{\mathrm{d}t} = 1, \tag{11}$$

$$\frac{\mathrm{d}C_g}{\mathrm{d}t} = \mu_{gly}(F_g - C_g) - \mu_c C_g + \frac{p_{EA} E A_g}{1 + K A_g}, \tag{12}$$

$$\frac{\mathrm{d}A_g}{\mathrm{d}t} = \frac{\mu_c p_{AC}}{p_{CA}} C_g - \mu_T A_g + p_{SA} A_c - \frac{p_{EA} p_{AC} E A_g}{p_{CA}(1 + K A_g)} \tag{13}$$

$$v\frac{\mathrm{d}C_c}{\mathrm{d}t} = p_{AC} A_c - p_{CA} C_c - \frac{p_{bio} C_c}{1 + H_{gib} C_g + H_{aib} A_c} + p_{SC} S_c, \tag{14}$$

$$v\frac{\mathrm{d}A_c}{\mathrm{d}t} = p_A(S_c - A_c) + p_{AC}(C_c - A_c) + \frac{p_A \mu_T}{p_{SA}} A_g, \tag{15}$$

$$v\frac{\mathrm{d}S_c}{\mathrm{d}t} = \mu_s \left(C_g - S_c - \frac{p_{TCA} S_c}{1 + H_{gis} C_g + H_{ais} A_c} \right), \tag{16}$$

where the new nondimensional parameters are given by

$$p_{AC} = \frac{q_{AC}}{\beta}, \qquad p_{CA} = \frac{q_{CA}}{\beta}, \qquad p_{bio} = \frac{q_{bio}}{\beta}, \qquad p_{SA} = \frac{q_{SA} k_{gly} q_{AC}}{\beta q_{CA}(\lambda_s + q_{SA} + q_{SC})},$$
$$p_{SC} = \frac{q_{SC} q_A q_{CA}}{\beta q_{SA} q_{AC}}, \qquad p_A = \frac{q_A}{\beta}, \qquad \mu_{gly} = \frac{k_{gly}}{\beta}, \qquad \mu_c = \frac{k_c}{\beta}, \qquad p_{TCA} = \frac{q_{TCA}}{\beta},$$
$$\gamma = \frac{\Gamma}{\beta}, \qquad H_{gis} = h_{gis} J_f, \qquad H_{gib} = h_{gib} J_f, \qquad H_{ais} = \frac{h_{ais} q_{SA} J_f}{q_A(q_{SA} + q_{SC} + \lambda_s)},$$
$$H_{aib} = \frac{h_{aib} q_{SA} J_f}{q_A(q_{SA} + q_{SC} + \lambda_s)}, \qquad \mu_s = \frac{\lambda_s + q_{SA} + q_{SC}}{\beta}, \qquad \mu_T = \frac{k_T}{\beta},$$
$$K = \frac{J_f q_{CA}}{K_E k_{gly} q_{AC}}, \qquad p_{EA} = \frac{k_{EA} J_E q_{CA}}{K_E \beta^2 q_{AC}}. \tag{17}$$

2.2 Examples of results

In the absence of concrete flux data to parameterise the model, we simply start by choosing all nondimensional parameters (17) equal to unity. Later we will vary some parameters with the aim of obtaining a set which roughly reproduce the qualitative features displayed in Table 1. By this, we mean a lower free acetate and a higher acetyl-CoA in the mutant at some time point. The system of equations was solved using Octave [10] (a Gnu Free Software Foundation version of matlab).

In Figure 5 we plot the glyoxysome concentrations in arbitrary units of time and concentration. Figure 6 shows the corresponding concentration in the cytosol. In both cases the left-hand graph is for the wildtype (Case A) and the right-hand graph the mutant (Case B). For the wild-type Case A, all parameters are unity except for $k_T = 0$ ($\mu_T = 0$); and in Case B, all are unity except for J_E, h_{ais}, h_{gis}, h_{aib}, h_{gib}, which are all zero.

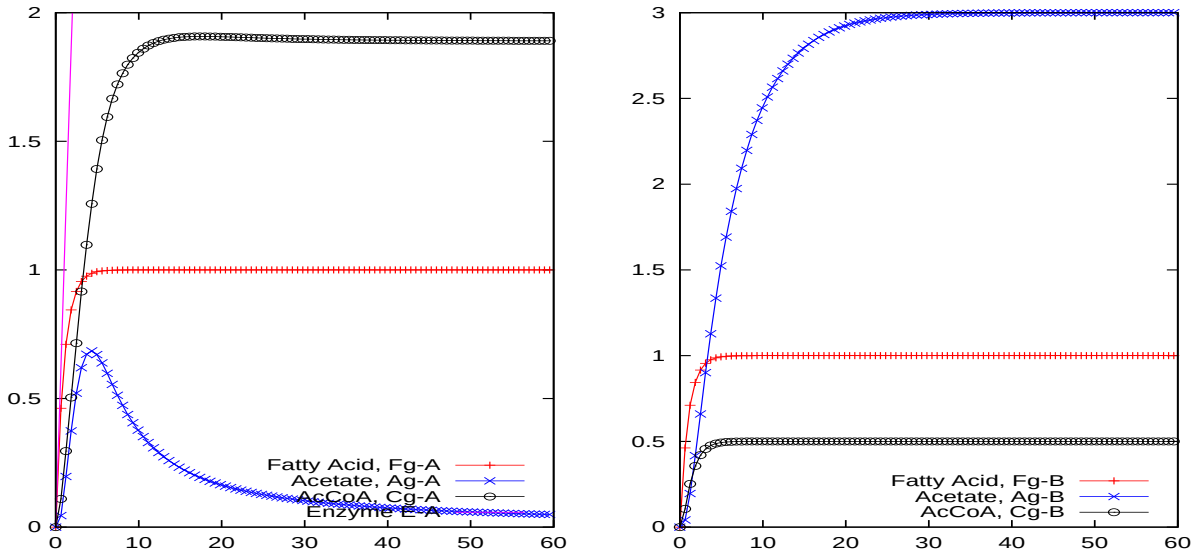

Figure 5: Concentrations of fatty acid, acetate, and acetyl-CoA in the glyoxysome plotted against time. Results from the deterministic model for the wildtype (Case A, left) and the mutant (Case B, right).

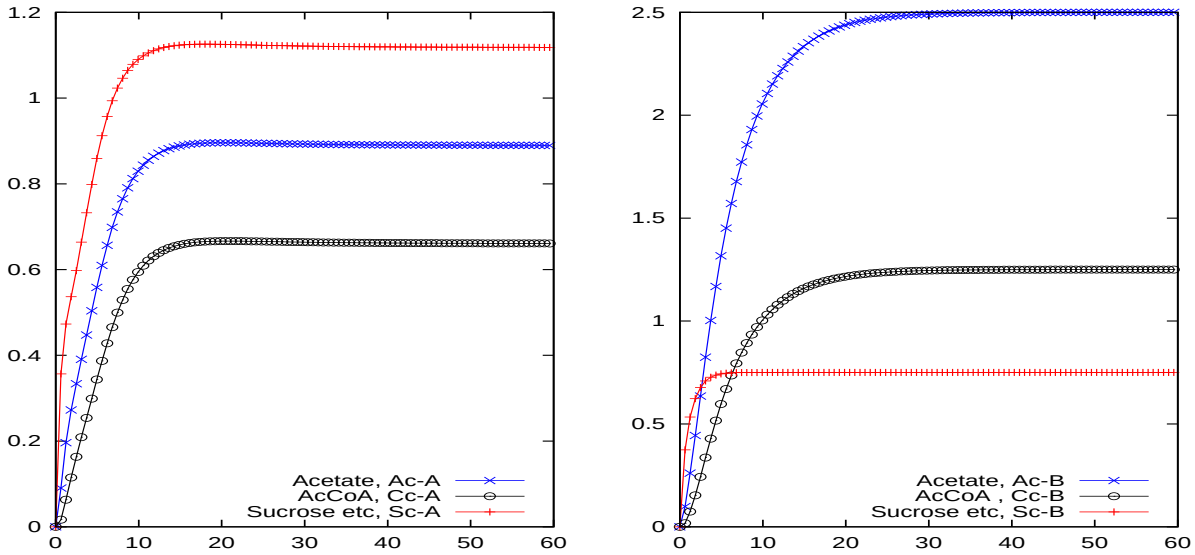

Figure 6: Concentrations of acetate, acetyl-CoA and sucrose (as an illustration of other metabolites) plotted against time. Results from the deterministic model for the wildtype (Case A, left) and the mutant (Case B, right).

2.3 Stochastic formulation and simulation results

In conjunction with the deterministic mathematical model a stochastic computational model was also developed. There were several reasons for doing this. Firstly, implementing the proposed model using two different approaches provides a check that each approach has been implemented correctly. For large numbers of molecules, the deterministic and stochastic models should agree, and, as we show below, this was indeed the case. Secondly, for cases where the number of molecules of any molecular species is small, deterministic models are no longer able to accurately predict the dynamics of the system being modelled. Rather, a stochastic modelling approach needs to be used. At this time, there are limited data on metabolite levels and flux values to fit to model parameters. If genetic regulatory mechanism are included in the model (for example, genetic regulation of the sucrose production pathway or biosynthesis pathway) then stochastic effects will need to be taken into account.

To implement the model we used a stochastic P system framework [9]. The model was designed graphically in CellDesigner. Using this approach, model design is very straightforward and biologist-friendly, and simply a case of drawing a reaction diagram using certain conventions. Two models were implemented: one without regulation of the sucrose and biosynthesis pathways, and one with. The models are shown in Figures 7 and 8. Once implemented, the model is saved using SBML, a standard computer-readable format for encoding systems biology models. The model was then executed using mcss, a freely-available multicompartment stochastic simulator. Since the values for the reaction constants are generally unavailable from biological data, in the initial models all stochastic reaction constants were set to 1. For each model, the *acn1* mutant is simulated by setting the initial number of ACN1p molecules to 0, as opposed to 1 in the wildtype.

Results from a single run of the stochastic model without genetic regulation are shown in Figure 9. As can be seen, the levels of the molecules are noisy. A clearer picture of

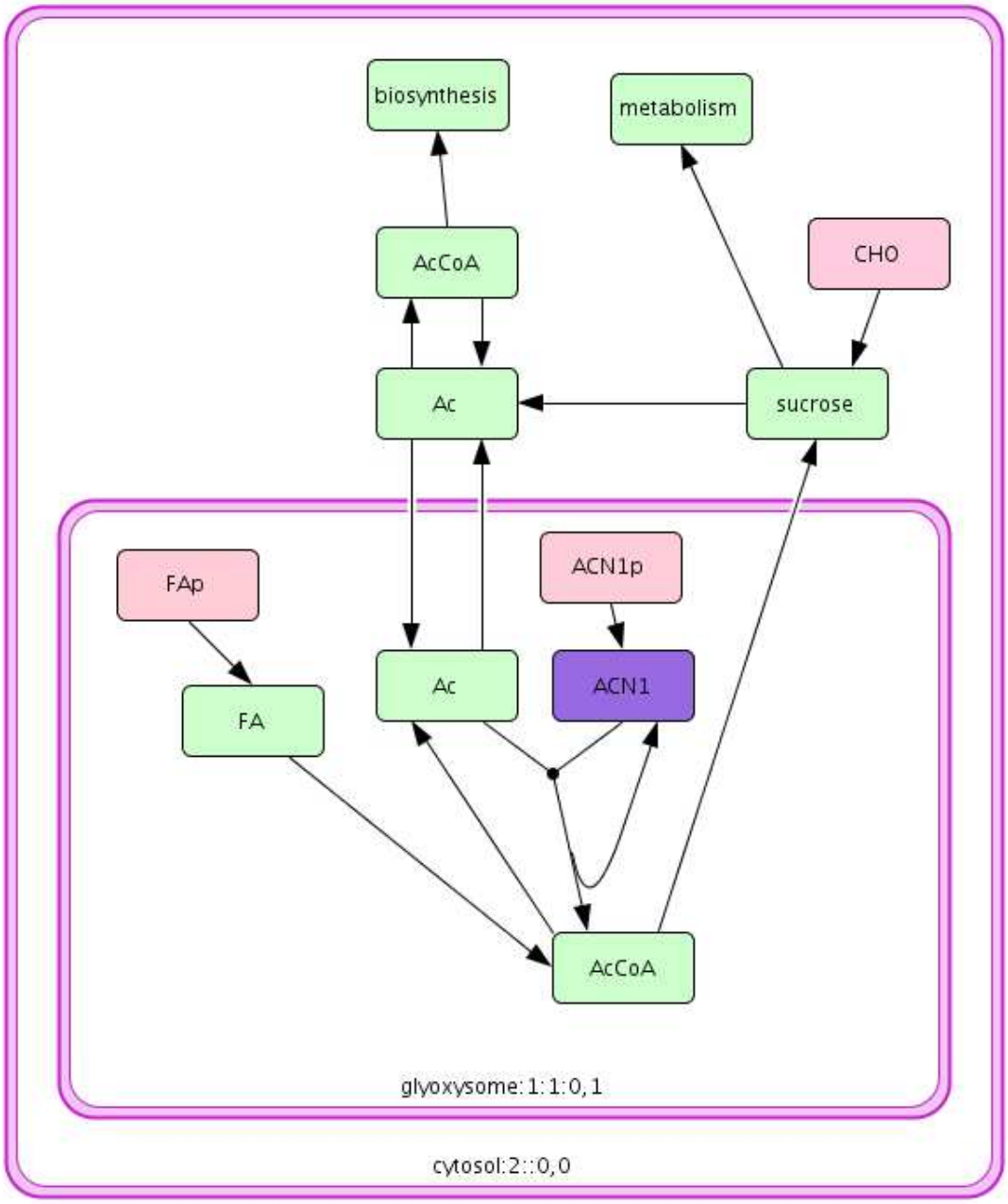

Figure 7: The stochastic computational model implementation *without* regulation of the sucrose and biosynthesis pathways.

the average behaviour of the system can be gained from running the model a number of times and calculating the average levels. Figure 10 shows the average levels over 10,000 runs for the wildtype and *acn1* mutant models without genetic regulation. Comparing with the results for the deterministic model in Figure 5, good agreement can be seen. It is clear from the plots in both Figures 5 and 10 that the results of the model are opposite that of the experimental observations. However, there are other suitable hypotheses that can be imposed to refine the model (and its parameterisation).

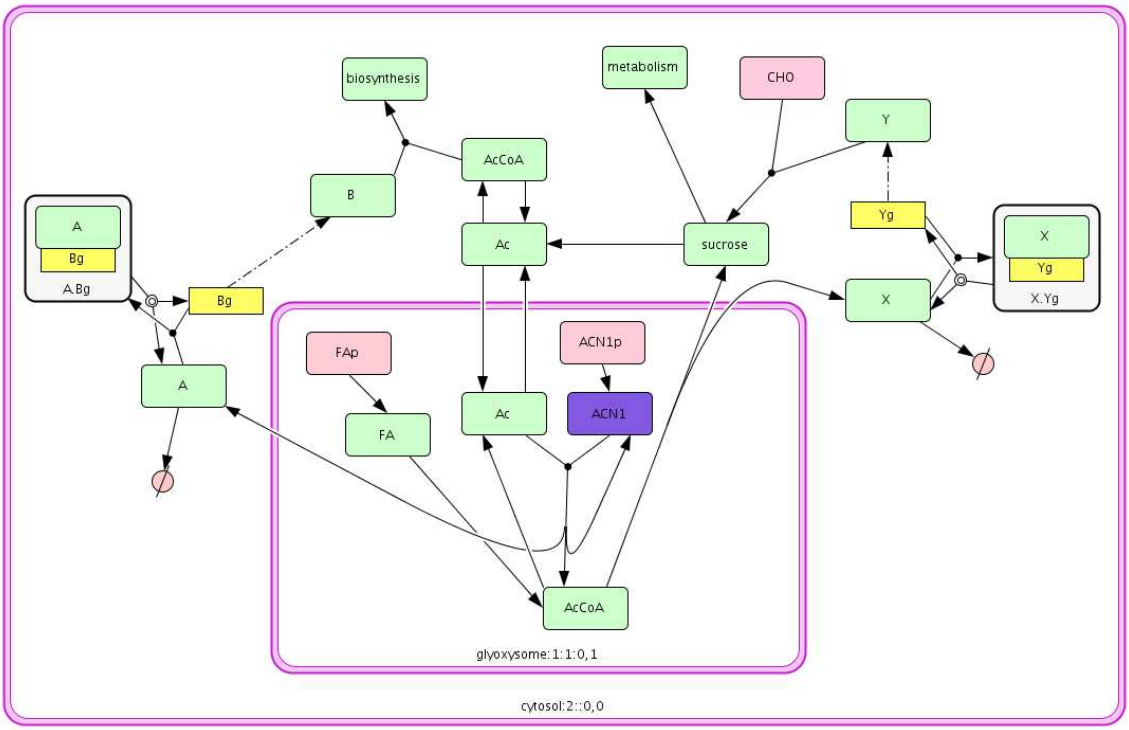

Figure 8: The stochastic computational model implementation *with* regulation of the sucrose and biosynthesis pathways.

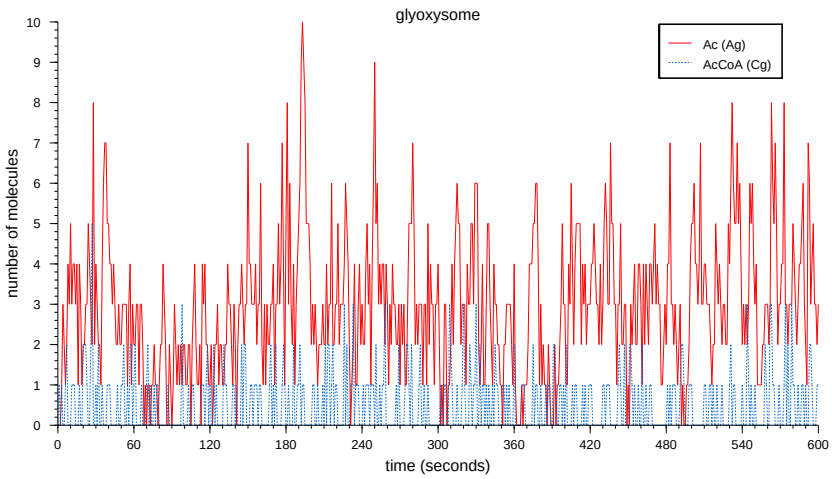

Figure 9: A single simulation run for the stochastic *acn1* mutant model without genetic regulation. The figure shows the number of molecules for two different species in the glyoxysome. From the figure it can be seen that the number of molecules does not stay constant, but fluctuates over time.

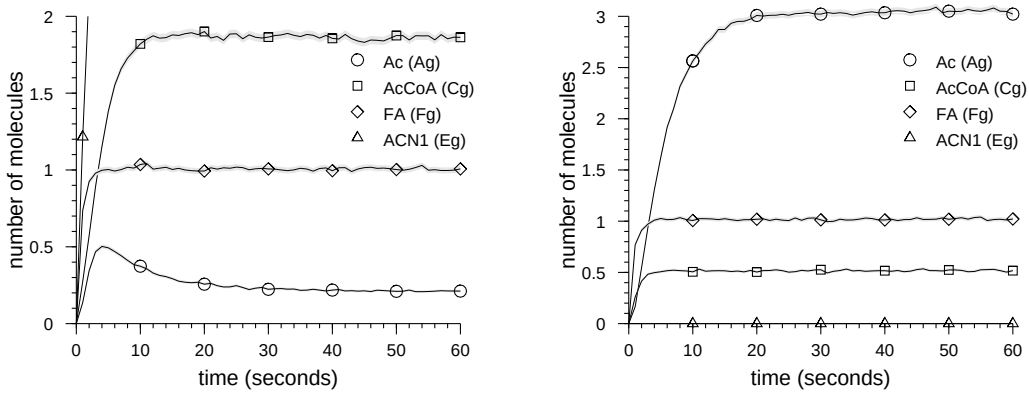

Figure 10: Left: average species levels in the glyoxysome for the stochastic wildtype model without genetic regulation. Right: similar for the *acn1* mutant model without genetic regulation. Confidence intervals are given as pink ranges.

3 Steady-state hypotheses

In days 2–4, the flux into F_g is approximately constant and the activity of the glyoxylate cycle is at its maximum and changes very little. Thus during this time, it is reasonable to consider a steady-state solution of the system of equations (11)–(16).

We have noted above that the volume ratio v is large, having a value in the range 10–100. We use this fact to simplify the dynamics, since it implies that the chemical reactions occurring in the glyoxysome will equilibrate much faster than those in the cytosol. We simplify the system of equations by assuming that the chemical species in the glyoxysome are at a 'local' equilibrium defined by the fluxes in and out from the cytosol.

3.1 Special Case A - wild-type pseudo-steady-state

For the wildtype, we assume that the inhibition is explicitly due to acetyl-CoA in the glyoxysome and not acetate in the cytosol, and hence put $H_{aib} = 0 = H_{ais}$. However, our analysis will show a close resultant link between C_g and A_c. Furthermore, we ignore the TE enzymatic export of acetate out of the glyoxysome, this corresponds to putting $\mu_T = 0$; but we retain the enzymatic conversion of acetate to acetyl-CoA in the glyoxysome.

Hence we start from the equations

$$\frac{\mathrm{d}F_g}{\mathrm{d}t} = \exp(-\gamma t) - F_g, \qquad \frac{\mathrm{d}E}{\mathrm{d}t} = 1, \tag{18}$$

$$\frac{\mathrm{d}C_g}{\mathrm{d}t} = \mu_{gly}(F_g - C_g) - \mu_c C_g + \frac{p_{EA} E A_g}{1 + K A_g}, \tag{19}$$

$$\frac{\mathrm{d}A_g}{\mathrm{d}t} = \frac{\mu_c p_{AC}}{p_{CA}} C_g + p_{SA} A_c - \frac{p_{EA} p_{AC} E A_g}{p_{CA}(1 + K A_g)} \tag{20}$$

$$v\frac{\mathrm{d}C_c}{\mathrm{d}t} = p_{AC} A_c - p_{CA} C_c - \frac{p_{bio} C_c}{1 + H_{gib} C_g} + p_{SC} S_c, \tag{21}$$

$$v\frac{\mathrm{d}A_c}{\mathrm{d}t} = p_A(S_c - A_c) + p_{AC}(C_c - A_c), \tag{22}$$

$$v\frac{\mathrm{d}S_c}{\mathrm{d}t} = \mu_s \left(C_g - S_c - \frac{p_{TCA} S_c}{1 + H_{gis} C_g} \right). \tag{23}$$

The large size of v means that the system responds on two timescales, a fast one over which F_g, C_g, A_g reach a local steady-state, and a longer/slow timescale during which C_c, A_c and S_c evolve. To simplify the system, let us consider only the longer timescale, and assume that the dynamics of F_g, C_g, A_g are at their steady-states. For this to be valid, we require γ to be small ($\gamma \sim 1/v$); then we have

$$C_g = F_g + \frac{p_{SA} p_{CA} A_c}{\mu_{gly} p_{AC}}, \qquad F_g = \exp(-\gamma t), \tag{24}$$

$$A_g = \frac{p_{SA} p_{CA}(\mu_c + \mu_{gly}) A_c + \mu_c p_{AC} \mu_{gly} F_g}{p_{EA} p_{AC} E_1 \mu_{gly} - K p_{SA} p_{CA}(\mu_c + \mu_{gly}) A_c - K \mu_c p_{AC} \mu_{gly} F_g}. \tag{25}$$

However, in the ensuing analysis, we will, more simply, assume that F_g takes some value, and express all other concentrations in terms of F_g.

In order for the expression (25) to be physically relevant, we require K to be below some threshold. Hence let us make the further simplifying assumption, that K is asymptotically small, and then we have

$$A_g = \frac{\mu_c F_g}{p_{EA} E_1} + \frac{p_{SA} p_{CA}(\mu_c + \mu_{gly}) A_c}{p_{EA} p_{AC} E_1 \mu_{gly}}. \tag{26}$$

The reduced system for A_c, C_c, S_c is then

$$v\frac{\mathrm{d}A_c}{\mathrm{d}t} = p_A(S_c - A_c) + p_{AC}(C_c - A_c), \tag{27}$$

$$v\frac{\mathrm{d}C_c}{\mathrm{d}t} = p_{AC} A_c - p_{CA} C_c - \frac{p_{bio} C_c}{1 + H_{gib} F_g + H_{gib} p_{SA} p_{CA} A_c / p_{AC} \mu_{gly}} + p_{SC} S_c, \tag{28}$$

$$v\frac{\mathrm{d}S_c}{\mathrm{d}t} = \mu_s \left(F_g + \frac{p_{SA} p_{CA} A_c}{\mu_{gly} p_{AC}} - S_c - \frac{p_{TCA} S_c}{1 + H_{gis} F_g + H_{gis} p_{SA} p_{CA} A_c / p_{AC} \mu_{gly}} \right). \tag{29}$$

Although we put $H_{ais} = 0 = H_{aib}$ earlier to remove the explicit inhibition of the biosynthesis and citric acid cycle processes by acetate in the cytosol, we find that this separation

of timescales, links acetate in the cytosol with acetyl-CoA in the glyoxysome through (24). Hence we find inhibition by acetate in the cytosol is implicit in the reduced model (27)–(29).

Fitting the reduced model (27)–(29) to experimental data might be simpler than the full model (18)–(23), since there are fewer parameters to determine. Further simplifications can be made by assuming that the inhibited pathways are completely shut down ($H_{gis}, H_{gib} \to \infty$), we would then obtain

$$v\frac{\mathrm{d}A_c}{\mathrm{d}t} = p_A(S_c - A_c) + p_{AC}(C_c - A_c), \tag{30}$$

$$v\frac{\mathrm{d}C_c}{\mathrm{d}t} = p_{AC}A_c - p_{CA}C_c + p_{SC}S_c, \tag{31}$$

$$v\frac{\mathrm{d}S_c}{\mathrm{d}t} = \mu_s\left(F_g + \frac{p_{SA}p_{CA}A_c}{\mu_{gly}p_{AC}} - S_c\right). \tag{32}$$

If we assume that these reactions are also at steady-state (and hence governed by the input of fatty acids into the entire system) we find

$$A_c = \frac{(p_{SC}p_{AC} + p_A p_{CA})p_{AC}\mu_{gly}F_g}{\mu_{gly}p_{AC}p_{CA}p_A + \mu_{gly}p_{AC}^2 p_{CA} - \mu_{gly}p_{AC}^3 - p_A p_{CA}^2 p_{SA} - p_{SC}p_{AC}p_{SA}p_{CA}}, \tag{33}$$

$$C_c = \frac{(p_A p_{AC} + p_{SC}p_A + p_{SC}p_{AC})p_{AC}\mu_{gly}F_g}{\mu_{gly}p_{AC}p_{CA}p_A + \mu_{gly}p_{AC}^2 p_{CA} - \mu_{gly}p_{AC}^3 - p_A p_{CA}^2 p_{SA} - p_{SC}p_{AC}p_{SA}p_{CA}}, \tag{34}$$

$$S_c = \frac{(p_A p_{CA} + p_{CA}p_{AC} - p_{AC}^2)p_{AC}\mu_{gly}F_g}{\mu_{gly}p_{AC}p_{CA}p_A + \mu_{gly}p_{AC}^2 p_{CA} - \mu_{gly}p_{AC}^3 - p_A p_{CA}^2 p_{SA} - p_{SC}p_{AC}p_{SA}p_{CA}}, \tag{35}$$

Since the glyoxysome has a much smaller volume than the cytosol, the total acetate (A^A) and total acetyl-CoA (C^A) concentrations are basically the concentrations in the cytosol ($A^A \approx A_c$ and $C^A \approx C_c$ respectively). We will use these quantities later to compare results for the wildtype and the mutant.

3.2 Special Case B - the *acn1* mutant

In the case of the *acn1* mutant there is no enzyme production ($E = 0$) and no inhibition (all the parameters $H_* = 0$) but we do have acetate transport across the glyxoxysome membrace ($\mu_T > 0$). We assume that the input of fatty acids into the glyoxysome is balanced by the loss, and so is held at a constant level, with $F_g < 1$. Since $v \gg 1$, the concentrations in the glyoxysome C_g, A_g, F_g self-equilibrate faster than the cytosol concentrations (C_c, A_c and S_c). Thus (11)–(16) can be simplified.

Solving the steady-state equations (11)–(13) in the case $E = 0$, leads to

$$F_g = \exp(-\gamma t), \qquad C_g = \frac{\mu_{gly}F_g}{\mu_c + \mu_{gly}}, \tag{36}$$

$$A_g = \frac{p_{SA}A_c}{\mu_T} + \frac{\mu_c p_{AC}\mu_g lyF_g}{\mu_T p_{CA}(\mu_c + \mu_{gly})}. \tag{37}$$

Equations (14)–(16), with all the inhibition switched off ($H_* = 0$) then imply

$$v\frac{\mathrm{d}A_c}{\mathrm{d}t} = p_A S_c + p_{AC}(C_c - A_c) + \frac{p_A \mu_c p_{AC} \mu_{gly} F_g}{p_{SA} p_{CA}(\mu_c + \mu_{gly})}, \tag{38}$$

$$v\frac{\mathrm{d}C_c}{\mathrm{d}t} = p_{AC}A_c - p_{CA}C_c - p_{bio}C_c + p_{SC}S_C, \tag{39}$$

$$v\frac{\mathrm{d}S_c}{\mathrm{d}t} = \mu_s\left(\frac{\mu_{gly}F_g}{\mu_c + \mu_{gly}} - S_c + p_{TCA}S_C\right). \tag{40}$$

If we seek the steady-state solution of (38)–(40) we find

$$A_c = \left(\frac{p_{SC}p_{bio}/(p_{CA} + p_{bio}) + p_A p_{bio}/p_{AC}}{(p_{CA} - p_{AC} + p_{bio})(1 - p_{TCA})} + \frac{p_A\mu_c}{p_{SA}p_{CA}}\right)\frac{\mu_{gly}F_g}{(\mu_c + \mu_{gly})}, \tag{41}$$

$$C_c = \left(\frac{p_{SC}p_{bio}/(p_{CA}+p_{bio}) + p_A p_{bio}}{(p_{CA}-p_{AC}+p_{bio})(1-p_{TCA})} + \frac{p_{AC}p_A\mu_c}{p_{SA}p_{CA}} + \frac{p_{SA}}{(1-p_{TCA})}\right)\frac{\mu_{gly}F_g}{(\mu_c+\mu_{gly})(p_{CA}+p_{bio})}, \tag{42}$$

$$S_c = \frac{\mu_{gly}F_g}{(\mu_c + \mu_{gly})(1 - p_{TCA})}. \tag{43}$$

This implies some constraints on parameter values, for example $p_{TCA} < 1$, in order for a physically realisable steady-state solution to exist.

4 Discussion

4.1 Comparison of results

Following a later meeting with Mark Hook, the model was refined and parameter values adjusted. We aimed to find rate constants which give rise to qualitatively similar behaviour to that reported in Table 1. We compare the total acetate concentrations in the wildtype (A^A) with that in the mutant (A^B), and repeat for the total acetyl-CoA (C^A and C^B). In Figure 11 we plot all the concentrations in the model against time for both the wildtype and the mutant to allow direct comparison of all calculated quantities. All curves are seen to increase from zero, saturate and then decline. In the mutant, these are smooth, with a slower decline. In the wildtype, we observe more interesting dynamics, as the balance between the reactions changes due to the increasing levels of enzyme present in the glyoxysome.

Since it is impossible or extremely difficult to measure any of the quantities plotted in Figure 11, we combine them into the observables of total acetate and total acetyl-CoA in the seedling via

$$A = A_c + \frac{A_g}{v}, \qquad C = C_c + \frac{C_g}{v}. \tag{44}$$

and these quantities are plotted in Figure 12 on a log-log-scale. This graph shows that for certain choices of parameter values it is possible to simultaneously achieve wildtype

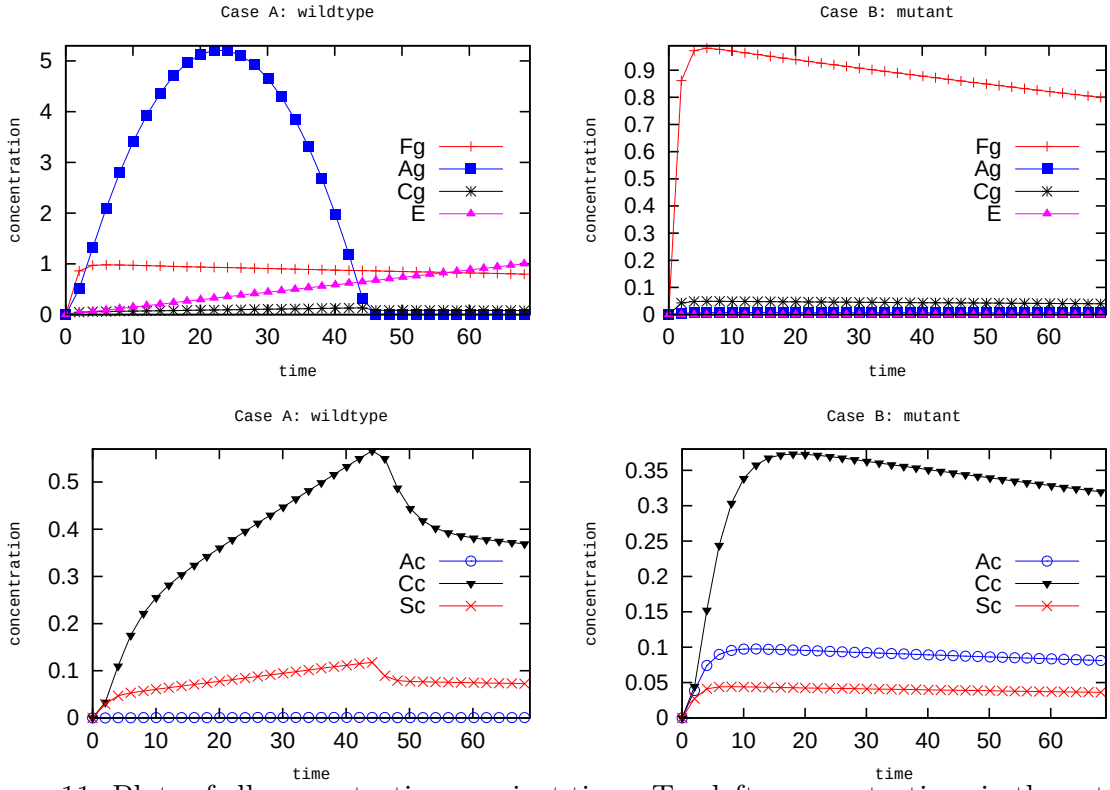

Figure 11: Plots of all concentrations against time. Top left: concentrations in the cytosol for the wildtype ; bottom left: concentrations in the glyoxysome for the wildtype ; top right: concentrations in the cytosol for the mutant; bottom right: concentrations in the glyoxysome for the mutant. Note that all graphs have different vertical scales. Parameter values: $k_c = 10$, $k_{EA} = 0.01$, $JF = 1$, $\beta = 1$, $K_E = 1$, $q_A = 5$, $k_{gly} = 10$, $v = 10$, $q_{AC} = 5$, $q_{CA} = 0$, $q_{SC} = 1.5$, $q_{bio} = 3$, $\lambda_S = 10$, $J_F = \exp(-t/300)$, $h_{gis} = 0 = h_{ais} = h_{gib} = h_{aib}$, $q_{TCA} = 1$. In addition, for Case A (wildtype), we have $k_T = 0$, $J_E = 4.1$; whereas in case B (the mutant *acn1*) we put $k_T = 130$, $J_E = 0$.

acetate exceeding acetate in the mutant and acetyl-CoA in the mutant exceeding acetyl-CoA in the wildtype.

In Figure 12 we note that at early times, acetyl-CoA in the mutant exceeds that in the wildtype, with both increasing at a similar rate. However, at later times the mutant saturates, and the wildtype continues to increase, peaks and then falls. The situation for total acetate concentrations is similar: both wildtype and mutant increase at early times, the mutant saturates earlier than the wildtype. At later times the increase in the wildtype is stopped at about $t = 45$ ($\log t = 3.8$) as the enzyme in the glyoxysome completes its conversion of acetate into acetyl-CoA. The consequential reduction of acetate takes the wildtype's concentration below that in the mutant. There is a noticable sudden reduction in acetyl-CoA in the wildtype, but this remains above the level of acetyl-CoA in the mutant.

Figure 11 suggests that a steady-state assumption may be valid for the mutant, since for $t > 10$ all concentrations appear to be evolving very slowly. However, the curve for acetate in the glyoxysome (A_g) in the upper left graph suggests that a steady-state assumption for the wildtype is not valid. At early times, there is a build-up of acetate

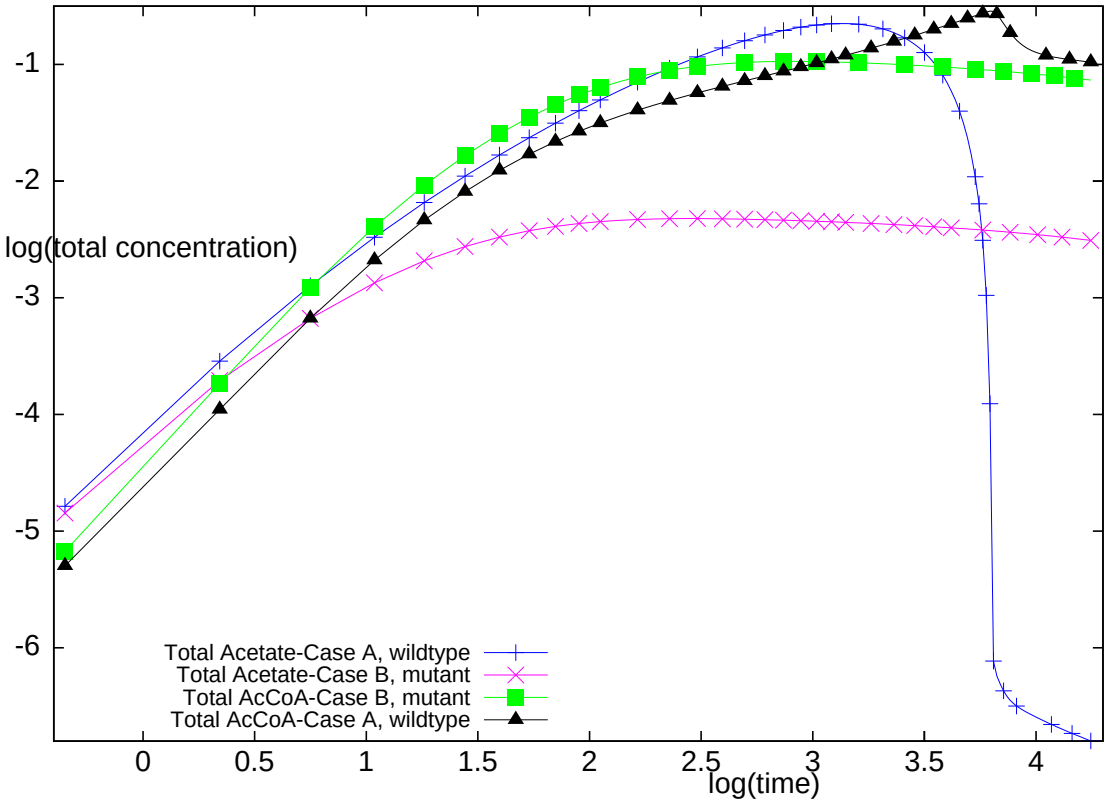

Figure 12: We plot the natural logaritgm of the total acetate and total acetyl-CoA concentrations against the logarithm of time. The lines marked with '+' signs and with triangles correspond to the total acetate and total acetyle CoA concentrations in the wildtype. The lines marked with 'x' signs and with squares correspond to the total acetate and total acetyl CoA concentrations in the *acn1* mutant respectively. Parameter values: $k_c = 10$, $k_{EA} = 0.01$, $JF = 1$, $\beta = 1$, $K_E = 1$, $q_A = 5$, $k_{gly} = 10$, $v = 10$, $q_{AC} = 5$, $q_{CA} = 0$, $q_{SC} = 1.5$, $q_{bio} = 3$, $\lambda_S = 10$, $J_F = \exp(-t/300)$, $h_{gis} = 0 = h_{ais} = h_{gib} = h_{aib}$, $q_{TCA} = 1$. In addition, for Case A (wildtype), we have $k_T = 0$, $J_E = 4.1$; whereas in case B (the mutant *acn1*) we put $k_T = 130$, $J_E = 0$.

(and other species), and at later times a rapid loss of acetate due to the enzyme concentration reaching a level where it converts acetate to acetyl-CoA. After this stage, there may be a steady-state, but by this time, the seedling will have started deriving energy from photosynthesis.

4.2 Conclusions

We have constructed a general model for the metabolic pathways in *Arabidopsis* seedlings. In particular we have identified the dominant pathways in two variants: the wildtype Columbia-7 and the mutant, *acn1*. We have constructed steady-state solutions for both cases, and solved the dynamical system for the time-dependent problem with crude guesses for all rate parameters.

These guesses have shown that the counterintuitive behaviour observed in some exper-

iments can be accounted for by the model equations. Despite the mutant lacking the enzyme which converts acetate into acetyl-CoA, the mutant exhibits higher total acetyl-CoA than the wildtype and lower acetate. The reason for this result is that the enzyme is only operative inside the glyoxysome; in the cytosol (outside the glyoxysome) different reaction mechanisms involving acetate and acetyl-CoA are active. By adjusting the rate parameters of all the processes occuring, it is possible to reproduce the experimentally observed behaviour in the deterministic model.

We have also implemented a stochastic model whose expected behaviour has been shown to mimic exceedingly well that of the deterministic model. Whilst the small size of the glyoxysome means that there are relatively few molecules in any one glyoxysome at any one time; due to the vast number of cells present in a seedling, the determinstic model gives a good representation of the experimental data.

Let us now review the questions posed in the introduction and suggest some responses.

Questions:

1. Why is free acetate lower, but acetyl-CoA higher within the *acn1* mutant ?

This is the counterintuitive reduction in acetate in the mutant which lacks the enzyme responsible for converting acetate to coA in the glyoxysome. The reason for this must be that in the mutant, acetate is then exported out of the glyoxysome by the enzyme TE, and in the cytosol, acetate is converted to into acetyl-CoA. In the wildtype, acetate is manufactured through the $F_g - C_g - S_c - A_c - A_g$ pathway; however, in the *acn1* mutant, this pathway is less active, instead, there is the $F_g - C_g - A_g - A_c$ pathway which also gives rise to the production of acetate. The effect of q_{AC} is to lower A_c (cytosol levels of acetate) which reduces the flux of acetate into the glyoxysome, and hence the acetyl-CoA in the glyoxysome also.

2. Why does the elimination of ACN1 have a large reductive effect on metabolite levels ?

Removal of acetyl-CoA by TE (high k_c) would decrease k_{gly} thereby impacting metabolite levels and gluconeogenesis (q_{TCA}).

3. Does acetyl-CoA from free acetate mimic acetyl-CoA pools derived from fatty acid catabolism ?

We see no reason to treat the two sources of acetyl-CoA separately. However, we would advise that models of the process treat acetate and acetyl-CoA in the cytosol separately from that in the glyoxysome, since different reactions occur in the two locations.

4. Must acetate and fatty acids share common metabolic pathways and isozymes ?

This is not a question we could address using the model. More information on metabolite levels and flux values using metabolic mutants is essential to answer this question.

5. What, if any, is the contribution of acetate recycling to metabolite levels, for example, is it possible that $q_{SC} = 0$?

Yes, q_{SC} could be zero, particularly if the alternative mechanisms given by the rates q_{SC} and q_{CA} are nonzero; these processes denote the conversion of metabolites through the citric acid cycle to acetyl-CoA in the cytosol and from there to acetate.

6. What is the contribution of cytosolic sources to acetate and acetyl-CoA levels ?

q_{AC} is necessary to produce acetyl-CoA and reduce acetate. q_{SC} can be zero which implies that there does not have to be a large net flux of metabolites to acetyl-CoA. However, the extra freedom allowed by $q_{SC} > 0$ allows for a more accurate fit to the experimental data, but a reasonable fit can be achieved with $q_{SC} = 0$, that is, without recycling of acetate.

With more work, it may be possible to fit the data more accurately. The model has illustrated the need to find more data from a series of time points. The system exhibits both fast and slow timescales, due to the dominant chemical reactions occuring in compartments of different sizes. Given more data for fitting parameter values, it would be interesting to derive and analyse a simplified model for the evolution of concentrations on the slower timescale.

4.3 Future work

The exercise presented here demonstrated that it is possible to derive models that fit the data thus far obtained by experimental characterization of the metabolism of the *acn1* mutant. These models provide clear direction for future work on metabolite flows in *Arabidopsis* seedlings. This future work will involve two discreet, but interactive programmes. One is continued refinement of mathematical models using published sources of data, and the other is the collection of data using a variety of experimental approaches to fit into the models.

Modelling

The model presented here addressed the question of what happens with acetate, acetyl-CoA, and metabolite levels if the peroxisomal acetyl-CoA synthetase is removed. Noting the position of this mutant in acetate metabolism, this model represents outcomes if glyoxysomal acetate metabolism is disrupted at a very early step. Certain assumptions have been made to reduce the complexity of the models, and these assumptions can be tested with information already at hand (for example, the pseudo-steady-state hypothesis). There are a number of other *Arabidopsis* mutant lines deficient in enzymatic steps involved in the model, such as isocitrate lyase [4], malate synthase [3], and malate dehydrogenase [12]. Initial characterization of these mutants using radio tracer feeding experiments has provided information on the assimilation of acetate into various classes of compounds. Such published data can be used to derive more localised/specific models of acetate flux through the glyoxylate cycle. Continuing work on models will involve regular visits among the modelling and experimental partners. As mentioned previously, one post-meeting visit has already taken place between Mark Hooks (Bangor University) and Jonathan Wattis (University of Nottingham) to work on initial model refinement and to formulate more detailed models. Furthermore, the models presented here will be supplemented with multivariate statistical modelling, such as metabolic network cartography in order to identify interesting interactions to include within models.

Experimentation

The radiolabelling experiments that have been routinely used to investigate acetyl-CoA metabolism in glyoxylate cycle and other mutants in seedlings have been useful, primarily to describe function for non-critical steps of seedling carbon metabolism. This data reveals how acetate is partitioned into classes of the classes of compounds representing respiration (CO2), intermediary metabolites (sugars, amino acids, organic acids), lipid and fatty acids, and insoluble end-products (proteins and complex carbohydrates). Such global information is well suited to initial model development as the number of parameters remains reasonable and the models not overly complex. However, such experiments do not provide the detailed information of metabolite partitioning that accurately describes acetate conversion, particularly within classes of compounds, such as among organic acids that are involved in both the glyoxylate and TCA cycles, for example. The experiments are also limited in the time frame they represent, since feeding experiments are usually done over the period of a few hours and at a particular stage of development. More detailed aspects of carbon flow can be elucidated by employing metabolomic means to measure metabolite levels in the various mutant backgrounds as well as more comprehensive radioisotope experimentation. Specific patterns of metabolite conversion over time using dynamic and steady-state stable isotope labelling will facilitate the evolution of mathematical models into detailed flux models. Therefore, the time scales of metabolism must also be considered in this respect. Model development can exploit certain stages of seedling growth where metabolism is essentially geared toward lipid catabolism, but critical metabolic changes may be happening at a number of different stages of development [5] (and personal communication with Allen & Hooks). Therefore, short (hours) and long (days) time courses must be included within investigations. It is evident that primary metabolism during seed germination and seedling establishment remains an exciting system — and an agronomically important one — that will only be resolved by a combination of state-of-the-art, high throughput experimental approaches and mathematical modelling.

References

[1] H Beevers. Metabolic production of sucrose from fat. *Nature* **191**, 433–36, (1961).

[2] DT Canvin & H Beevers. Sucrose synthesis from acetate in the germinating castor bean: kinetics and pathway. *J Biol Chem* **236**, 988–95, (1961).

[3] JE Cornah, V Germain, JL Ward, MH Beale & SM Smith. Lipid utilization, gluconeogenesis, and seedling growth in *Arabidopsis* mutants lacking the glyoxylate cycle enzyme malate synthase. *J Biol Chem*, **279**, 42916–42923, (2004).

[4] PJ Eastmond, V Germain, PR Lange, JH Bryce, SM Smith & IA Graham. Postgerminative growth and lipid catabolism in oilseeds lacking the glyoxylate cycle. *Proc Natl Acad Sci*, **97**, 5669–5674, (2000).

[5] A Fait, R Angelovici, H Less, I Ohad, E Urbanczyk-Wochniak, AR Fernie & G Galili. *Arabidopsis* seed development and germination is associated with temporally distinct metabolic switches. *Plant Physiology* **142**, 839–854, (2006).

[6] BL Fatland, BJ Nikolau & ES Wurtele. Reverse genetic characterization of cytosolic acetyl-CoA generation by ATP-citrate lyase in *Arabidopsis*. *Plant Cell* **17**, 182–203, (2005).

[7] IA Graham. Seed storage oil mobilization. *Annu Rev Plant Biol*, **59**, 115–42, (2008).

[8] MA Hooks, JE Turner, EC Murphy, KA Johnston, S Burr & S Jaroslawski. The *Arabidopsis* ALDP protein homologue COMATOSE is instrumental in peroxisomal acetate metabolism. *Biochem J* **406**, 399–406, (2007).

[9] MJ Pérez-Jiménez & FJ Romero-Campero. P systems, a new computational modelling tool for systems biology. *Transactions on Computational Systems Biology VI*, pp. 176–197, (2006).

[10] GNU Octave, Free Software Foundation, `http://www.gnu.org/software/octave`, (2009).

[11] I Pracharoenwattana, JE Cornah & SM Smith. *Arabidopsis* peroxisomal citrate synthase is required for fatty acid respiration and seed germination. *Plant Cell* **17**, 2037-48, (2005).

[12] I Pracharoenwattana, JE Cornah & SM Smith. *Arabidopsis* peroxisomal malate dehydrogenase functions in β-oxidation but not in the glyoxylate cycle. *The Plant Journal*, **50**, 381–390, (2007).

[13] JE Turner, K Greville, EC Murphy & MA Hooks. Characterisation of Arabidopsis Fluoroacetate-resistant mutants reveals the principal mechanism of acetate activation for entry into the glyoxylate cycle. *J Biol Chem*, **280**, 2780–2787, (2005).

[14] CW van Roermund, Y Elgersma, N Singh, RJ Wanders & HF Tabak. The membrane of peroxisomes in *Saccharomyces cerevisiae* is impermeable to NAD(H) and acetyl-CoA under *in vivo* conditions. *EMBO J*, **1414**, 3480–86, (1995).